Dicopper(I) Trefoil Knots and Related Unknotted Molecular Systems: Influence of Ring Size and Structural Factors on Their Synthesis and Electrochemical and Excited-State Properties

Christiane O. Dietrich-Buchecker,*[1a] Jean-François Nierengarten,[1a] Jean-Pierre Sauvage,*[1a] Nicola Armaroli,[1b] Vincenzo Balzani,*[1b] and Luisa De Cola[1b]

Contribution from the Laboratoire de Chimie Organo-Minérale, UA 422 au CNRS, Institut de Chimie, Université Louis Pasteur, F-67000 Strasbourg, France, and Dipartimento di Chimica "G. Ciamician", Università di Bologna, I-40126 Bologna, Italy

Received June 21, 1993[⊗]

Abstract: Five new dicopper(I) knots have been synthesized as well as their face-to-face isomers. The knots range from 80- to 90-membered rings, and their preparation yields depend crucially on structural parameters such as number of methylene fragments linking the two chelating units and length of the poly(ethyleneoxy) unit used in the cyclization reaction. The best yield was obtained for an 84-membered knotted ring with a $-(CH_2)_6-$ connector: this relatively long fragment allows pronounced winding of the double-helix precursor and is thus favorable to the knotting reaction. The face-to-face complexes were in some instances the major products, being obtained in yields amounting to 24% in the case of the dicopper(I) bis(43-membered-ring) system. The electrochemical properties of the copper complexes also depend on their structure. The redox potential values of the Cu(II)/Cu(I) couple span over a wide range (~0.5–0.75 V vs SCE), the most electrochemically stable copper(I) complex being the 84-membered knotted compound. In CH_2Cl_2 solution, both the Cu_2 knots and their face-to-face isomers exhibit metal-to-ligand charge-transfer absorption bands in the visible region and emission bands in the red spectral region. The profile of the absorption spectra and the luminescence properties (λ_{max}, quantum yield, lifetime, and rate of excited-state quenching by acetone) depend on the length of the connectors. In agreement with the electrochemical results, the $-(CH_2)_6-$ linker has a pronounced shielding effect on the metal center as well as a special ability to impose geometrical constraint.

Introduction

Although molecular knots were discussed in the chemical literature more than three decades ago,[2] it was only recently that the first chemical knot was synthesized.[3,4] The use of transition metals as assembling and templating species turned out to be crucial in the development of preparative methods allowing the synthesis of macroscopic amounts of catenanes and knots.[5,6] A recent report describes the experimental procedure for making the original dicopper knotted 86-membered ring as well as its face-to-face isomer complex, consisting of two 43-membered rings arranged around two copper(I) centers.[7]

In an attempt to improve the very poor yield (the dicopper trefoil knot was obtained in 3% yield only), some of us investigated the effect of structural parameters on the course of the reaction. The results obtained were recently reported as a preliminary communication.[8] We now report in more detail the preparative procedures used to obtain selected knotted and unknotted species, as well as to describe their electrochemical and excited-state properties.

Results and Discussion

Synthesis of the Complexes. The strategy[3] used is indicated in Figure 1. Figure 2 describes in a schematic way the alternative cyclization reaction leading to the unknotted face-to-face complexes and the equilibrium which interconverts the helical and the nonhelical precursors.

What will be determining is (i) the proportion of double-helix precursor formed versus face-to-face open-chain complex (Figure 2) and (ii) the spacial arrangement of the four reacting ends of the helicoidal dinuclear complex. This latter factor will reflect the degree of winding of the two molecular strings interlaced around the copper(I) atoms. The chemical structures of the starting compounds and the complexes synthesized and studied in the present paper are depicted in Figure 3a,b.

1,10-Phenanthroline was treated with *p*-lithioanisole[10] in ether at 0 °C to afford **1** in 69% yield after hydrolysis and oxidation by MnO_2. **2** was prepared by reacting **1** with methyllithium followed again by hydrolysis and oxidation; it was obtained as a white solid in 92% yield from **1**. The *bis*(phenanthroline) compound **3** was made by the oxidative coupling (iodine) of the deprotonation product generated from **2** and lithium diisopropylamide (LDA). It was obtained in good yield (77%) from **2**. **4** was prepared as previously described.[7] The bis-chelating ligand **5** was synthesized by reacting **1** with 1,6-dilithiohexane[11] in ether at 0 °C, followed by hydrolysis and MnO_2 treatment. **5** was obtained as a pale yellow solid in 60% yield.

⊗ Abstract published in *Advance ACS Abstracts*, October 15, 1993.

(1) (a) Université Louis Pasteur. (b) Università di Bologna.
(2) Frisch, H. L.; Wasserman, E. *J. Am. Chem. Soc.* **1961**, *83*, 3789.
(3) Dietrich-Buchecker, C. O.; Sauvage, J. P. *Angew. Chem., Int. Ed. Engl.* **1989**, *28*, 189.
(4) Dietrich-Buchecker, C. O.; Guilhem, J.; Pascard, C.; Sauvage, J. P. *Angew. Chem., Int. Ed. Engl.* **1990**, *29*, 1154.
(5) Dietrich-Buchecker, C. O.; Sauvage, J. P. *Bioorg. Chem. Front.* **1991**, *2*, 195. Sauvage, J. P. *Acc. Chem. Res.* **1990**, *23*, 319.
(6) Dietrich-Buchecker, C. O.; Sauvage, J. P. *New J. Chem.* **1992**, *16*, 277.
(7) Dietrich-Buchecker, C. O.; Sauvage, J. P.; Kintzinger, J. P.; Maltèse, P.; Pascard, C.; Guilhem, J. *New J. Chem.* **1992**, *16*, 931.
(8) Dietrich-Buchecker, C. O.; Nierengarten, J. F.; Sauvage, J. P. *Tetrahedron Lett.* **1992**, 3625.
(9) Walba, D. M. *Tetrahedron* **1985**, *41*, 3161.
(10) Gilman, H.; Zoellner, E. A.; Selby, W. M. *J. Am. Chem. Soc.* **1932**, *54*, 1957.
(11) West R.; Rochow, E. G. *J. Org. Chem.* **1953**, *18*, 1739. McDermott, J. X.; White, J. F.; Whitesides, G. M. *J. Am. Chem. Soc.* **1976**, *98*, 6529.

0002-7863/93/1515-11237$04.00/0

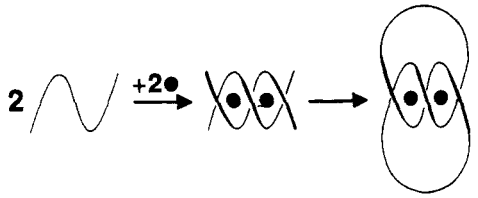

Figure 1. Principle of the strategy leading to a dimetallic trefoil knot. First step: interlacing of two molecular strings around two transition-metal coordinating centers, with formation of a helicoidal precursor. Second step: connection, with the appropriate linkers, between the four ends of the double helix to afford the knot.

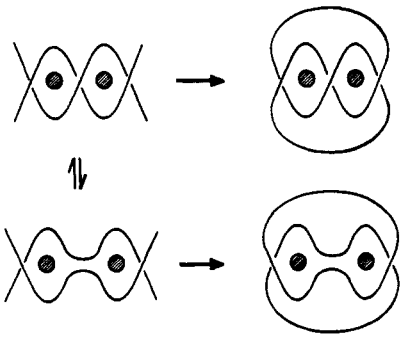

Figure 2. Equilibrium between the helicoidal interlaced system and its face-to-face analogous complex. Interconversion between the two isomeric cyclic products is of course not possible.

The three diphenols **6–8** were prepared following a demethylation procedure described earlier.[5,6,12] The anisyl derivative (**3–5**) was heated at ~200 °C in pyridinium chloride, followed by workup and careful drying. The yields were excellent (see Experimental Section) in spite of the brutal conditions used.

The dicopper(I) complexes $\mathbf{9^{2+}}$–$\mathbf{14^{2+}}$ were made by mixing $Cu(CH_3CN)_4^+$ with the corresponding diphenol (**6–8**). It must be stressed that mixtures of complexes were obtained, corresponding to the equilibrium of Figure 2. For instance, by preparing a stoichiometric mixture of **6** and $Cu(CH_3CN)_4^+ \cdot BF_4^-$ in DMF/CH_3CN (2:1, v/v), a mixture of $\mathbf{9^{2+}}$ and $\mathbf{12^{2+}}$ was obtained. Since the helicoidal complexes ($\mathbf{9^{2+}}$, $\mathbf{10^{2+}}$, and $\mathbf{11^{2+}}$) are in equilibrium with the corresponding face-to-face systems ($\mathbf{12^{2+}}$, $\mathbf{13^{2+}}$, and $\mathbf{14^{2+}}$, respectively), isolation of pure precursor complexes was not possible. In fact, although the equilibrium is slow on the ^{1}H-NMR time scale, reequilibration is expected to be fast under the conditions of the cyclization reaction, making any attempt to isolate pure samples of helicoidal or face-to-face precursors totally useless.

All the cyclization reactions leading to the dicopper trefoil knots $[\mathbf{Cu_2(k\text{-}82)}]^{2+}$ to $[\mathbf{Cu_2(k\text{-}90)}]^{2+}$ and the face-to-face dinuclear complexes $[\mathbf{Cu_2(m\text{-}40)_2}]^{2+}$ to $[\mathbf{Cu_2(m\text{-}45)_2}]^{2+}$ were carried out under similar conditions on the crude mixture of precursors (double-helix and face-to-face complexes). The phenolic complexes ($\mathbf{9^{2+}}$, $\mathbf{12^{2+}}$), ($\mathbf{10^{2+}}$, $\mathbf{13^{2+}}$), or ($\mathbf{11^{2+}}$, $\mathbf{14^{2+}}$) were reacted with the desired diiodo derivative (penta- or hexaethylene glycol) in DMF, in the presence of Cs_2CO_3, with vigorous stirring. After workup, the crude product had to be very thoroughly purified by repeated chromatography. The knotted and the face-to-face complexes were obtained in various proportions, depending on which open-chain compounds were used: bis(phenanthroline) **6–8** or diiodo derivative. The respective yields and characterizations are given in the Experimental Section (Tables VII–IX).

It can be noted that all the preparation yields are rather low, except for some face-to-face complexes which can be obtained in more than 20% yield. As far as dicopper(I) knots are concerned, the best result was obtained with $[\mathbf{Cu_2(k\text{-}84)}]^{2+}$ (8% yield). A possible explanation is that the $-(CH_2)_6-$ fragment linking the two phenanthroline units is particularly favorable either to double-helix versus face-to-face precursor formation or to cyclization to the knot. The latter explanation seems reasonable on the basis of a recent X-ray crystallographic study on $[\mathbf{Cu_2(k\text{-}84)}]^{2+}$.[13] The structure shows the helicoidal core to be very well adapted to the formation of a knot, particularly with a highly twisted helix, owing to the relatively long $-(CH_2)_6-$ fragment.

Electrochemical Properties. Some of the present complexes have been studied by cyclic voltammetry in CH_3CN. For comparison purposes, the electrochemical properties of the reference compound $[\mathbf{Cu(2)_2}]^+$ have also been investigated. The electronic properties of this mononuclear complex should be strictly identical to those of the other systems since each phenanthroline ligand bears one alkyl group and one anisyl-like substituent in all cases. Any difference between $[\mathbf{Cu(2)_2}]^+$ and the dinuclear knotted or unknotted complex can thus be attributed to *geometrical factors* and, in particular, to the geometry of the copper(I) coordination polyhedra and the accessibility to the metal centers.

Selected electrochemical data have been collected in Table I. It can be noted that, in the dinuclear compounds studied ($[\mathbf{Cu_2(k\text{-}84)}]^{2+}$, $[\mathbf{Cu_2(k\text{-}86)}]^{2+}$, and $[\mathbf{Cu_2(m\text{-}43)_2}]^{2+}$), the two copper(I) centers behave independently of one another.

Clearly, the acyclic complex $[\mathbf{Cu(2)_2}]^+$ is the easiest one to oxidize. This property reflects the small hindering and constraining character of the ligand set consisting of two open-chain chelates (**2**) coordinated to the copper(I) center.[14] By contrast, the redox potential of $[\mathbf{Cu_2(k\text{-}84)}]^{2+}$ is surprisingly high. It is even 140 mV higher than the redox potential of the other studied knot $[\mathbf{Cu_2(k\text{-}86)}]^{2+}$, which tends to indicate that the 84-membered knotted cycle is highly constraining and allows only limited freedom for the copper(I) centers to change their geometry. This observation is in perfect accordance with the structure of the compound.[13] The $-(CH_2)_6-$ linker is sufficiently long to form a well-twisted double helix in the central part of the molecule, ensuring efficient shielding of the metal centers. The pentaethylene glycol fragment is too short for the molecule to easily distort; the rigidity thus obtained "freezes" the copper centers in a pseudotetrahedral geometry and makes any deformation of their coordination polyhedra toward a square planar geometry extremely difficult.

Absorption Spectra and Luminescence Properties. (a) Excited States in $[Cu(NN)_2]^+$ Complexes. The compounds studied in this paper contain two $[Cu(phen)_2]^+$-type chromophoric units. Studies on the absorption spectra and luminescence properties of $[Cu(bpy)_2]^+$- and $[Cu(phen)_2]^+$-type species (hereafter indicated as $[Cu(NN)_2]^+$) have received a great deal of attention in the last fifteen years within the frame of the growing interest in the photochemical and photophysical properties of polypyridine transition-metal complexes.[15,16] Particularly important in this regard are the thorough investigations carried out by McMillin and co-workers since 1977.[17] In a series of papers,[17–28] they have

(12) Curphey, T. J.; Hoffman, E. J.; McDonald, C. *Chem. Ind.* **1967**, 1138.

(13) Albrecht-Gary, A. M.; Dietrich-Buchecker, C. O.; Guilhem, J.; Meyer, M.; Pascard, C.; Sauvage, J. P. *Recl. Trav. Chim. Pays-Bas Belg.* **1993**, *112*, 427.

(14) Federlin, P.; Kern, J. M.; Rastegar, A.; Dietrich-Buchecker, C. O.; Marnot, P. A.; Sauvage, J. P. *New J. Chem.* **1990**, *14*, 9.

(15) Juris, A.; Balzani, V.; Barigelletti, F.; Campagna, S.; Belser, P.; von Zelewsky, A. *Coord. Chem. Rev.* **1988**, *84*, 85.

(16) Kalianasundaram, K. *Photochemistry of Polypyridine and Porphyrin Complexes*; Academic Press: London, 1992.

(17) McMillin, D. R.; Buckner, M. T.; Ahn, B. T. *Inorg. Chem.* **1977**, *16*, 943.

(18) Ahn, B.-T.; McMillin, D. R. *Inorg. Chem.* **1981**, *20*, 1427.

(19) Kirchhoff, J. R.; Gamache, R. E., Jr.; Blaskie, M. W.; Del Paggio, A. A.; Lengel, R. K.; McMillin, D. R. *Inorg. Chem.* **1983**, *22*, 2380.

(20) Vante, N. A.; Ern, V.; Chartier, P.; Dietrich-Buchecker, C. O.; McMillin, D. R.; Marnot, P. A.; Sauvage, J. P. *Nouv. J. Chim.* **1983**, *7*, 3.

(21) McMillin, D. R.; Kirchhoff, J. R.; Goodwin, K. V. *Coord. Chem. Rev.* **1985**, *64*, 83.

(22) Phifer, C. C.; McMillin, D. R. *Inorg. Chem.* **1986**, *25*, 1329.

(23) Ichinaga, A. K.; Kirchhoff, J. R.; McMillin, D. R.; Dietrich-Buchecker, C. O.; Marnot, P. A.; Sauvage, J. P. *Inorg. Chem.* **1987**, *26*, 4290.

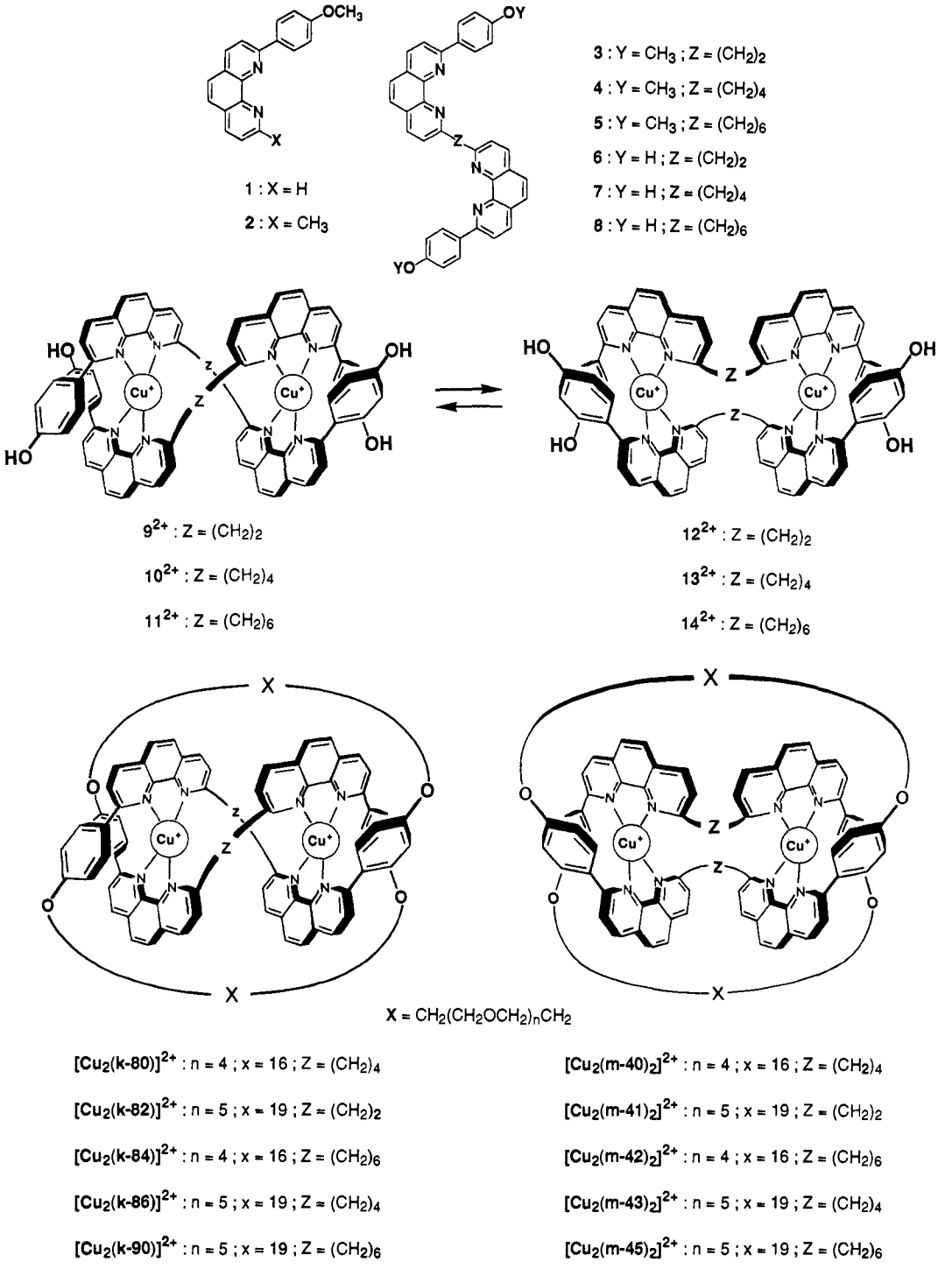

Figure 3. (a, Top) Acyclic precursors. (b, Bottom) Molecules described in the present report. For the cyclic compounds, the total number of atoms x connecting two phenolic oxygen atoms is 16 if $n = 4$ (pentakis(ethyleneoxy) fragment) or 19 if $n = 5$ (hexakis(ethyleneoxy) linker). Each knot is represented by the letter **k** accompanied by the overall number of atoms included in the cycle. The face-to-face complexes contain two monocycles (letter **m**), the number of atoms in each ring also being indicated. It can be noted that each knot has a face-to-face counterpart. For instance, $[Cu_2(k\text{-}90)]^{2+}$ and $[Cu_2(m\text{-}45)_2]^{2+}$ are constitutional isomers. *They are by no means topological stereoisomers.*[9]

examined the absorption and emission properties of a variety of $[Cu(NN)_2]^+$ complexes and have reached a satisfactory interpretation of their photophysical and photochemical behaviors.

Since Cu^+ can be easily oxidized and the NN-type ligands possess low-energy empty π^* orbitals, the visible absorption spectra of these complexes are dominated by metal-to-ligand charge-transfer (MLCT) bands. Even on the simplifying assumption of

Table I. Oxidation Potentials of Copper Mono- and Dinuclear Complexes[a]

	$[Cu(2)_2]^+$	$[Cu_2(k\text{-}84)]^{2+}$	$[Cu_2(k\text{-}86)]^{2+}$	$[Cu_2(m\text{-}43)_2]^{2+}$
E° vs SCE (V)	0.42	0.75	0.61	0.55[b]

[a] Cyclic voltammetry measurements in CH_3CN; $LiClO_4$ (0.1 M) as supporting electrolyte; oxidation on Pt; scan rate 100 mV/s; reference SCE. Most of the systems studied were found to be reversible (ΔE_p = 60 mV). [b] Irreversible oxidation.

(24) Gushurst, A. K. I.; McMillin, D. R.; Dietrich-Buchecker, C. O.; Sauvage, J. P. *Inorg. Chem.* **1989**, *28*, 4070.
(25) Everly, R. M.; McMillin, D. R. *Photochem. Photobiol.* **1989**, *50*, 711.
(26) Stacy, E. M.; McMillin, D. R. *Inorg. Chem.* **1990**, *29*, 393.
(27) Everly, R. M.; Ziessel, R.; Suffert, J.; McMillin, D. R. *Inorg. Chem.* **1991**, *30*, 559.
(28) Everly, R. M.; McMillin, D. R. *J. Phys. Chem.* **1991**, *95*, 9071.

a ground state D_{2d} symmetry, several symmetry-allowed MLCT transitions are possible from the e(xz,yz), $b_2(xy)$, $b_1(x^2-y^2)$, and $a(z^2)$ orbitals of the d^{10} Cu^+ ion to the accessible e(ψ), $a_2(\chi)$, and $b_1(\chi)$ π^* ligand orbitals (the z axis joins the metal and ligand centers). Further difficulties arise because of the broadness of the absorption (and luminescence) bands, which is related to the fact that the MLCT excited states are formally Cu^{2+} complexes and therefore prefer a higher coordination number.

As pointed out by McMillin *et al.*,[23-28] no more than three absorption bands are resolved in the spectra of the $[Cu(NN)_2]^+$ compounds. The most prominent one, indicated as band II, shows z polarization and can be associated with an $e(xz,yz) \rightarrow e(\psi)$ excitation. The maximum of this band lies in the 430–480-nm region, with a molar absorption coefficient of several thousand M^{-1} cm^{-1}. The higher energy band III which is absent in the bpy complex and exhibits xy polarization, lies around 390–420 nm and is often covered by the onset of the much more intense band II. Of particular interest is the lower energy band I, which in most cases appears as a shoulder above 500 nm. Parker and Crosby[29] have shown that band I has the same polarization as band II. Since there are only two z-polarized transitions allowed in D_{2d} symmetry, and one of them ($b_1(x^2-y^2) \rightarrow a_2(\chi)$) is expected to occur at much higher energy, the proposal has been advanced that band I corresponds to the $^1A_2$ term derived from the $e(xz,yz) \rightarrow e(\psi)$ excitation, which becomes z allowed under the influence of a D_2 flattening distortion.[29] In such a reduced symmetry, the lowest energy, z-polarized transition is $b_3(yz) \rightarrow b_2(\psi)$ and the relevant excited state is $^1B_1$.

The luminescence of the $[Cu(NN)_2]^+$ complexes can be assigned to low-energy MLCT levels. An important feature of such excited states is that the Cu^{2+} ion created by excitation is unsaturated in the original tetracoordinating environment and therefore these excited states show a great tendency to deactivate via formation of adducts (exciplexes).[21,25] Usually the luminescence spectrum at room temperature consists of a weak, broad band with a maximum at $\lambda > 700$ nm. A very peculiar aspect of this band is that both its energy and its intensity *decrease* with decreasing temperature. Since the luminescence lifetime increases at the same time, the only plausible explanation, as pointed out by McMillin and co-workers,[19] is that there are at least two emissive levels in thermal communication. In fact, subtraction of the 90 K spectrum from the higher temperature spectra yields a band which has its maximum at higher energy than that of the 90 K spectrum.[28] The energy gap between the two luminescent levels is of the order of 1000–2000 cm^{-1}. Estimated values of the respective radiative rate constants led McMillin *et al.* to assign the higher energy luminescent level as a singlet state and the lower energy one as a triplet state.[19,28] Since the luminescence bands are z polarized, group-theory arguments lead to the conclusion that the luminescent singlet is the $^1B_1$ level (in D_2 symmetry) responsible for the absorption band I, while the luminescent triplet $^3B_1$ derives from a different electronic configuration. Convincing evidence that the lowest MLCT excited state has the promoted metal electron localized on a single NN ligand was recently obtained by time-resolved resonance Raman spectroscopy.[30] This implies an excited-state distortion to a C_{2v} or C_2 symmetry but does not affect the conclusion that the thermally activated emission is associated with a singlet excited state.

Within the general frame underlined above, each $[Cu(NN)_2]^+$-type complex shows some peculiar features. In particular, substituents in the 2,9-positions of the phenanthroline ligand influence both the energy and the intensity of the MLCT absorption bands as well as the luminescence behavior. Steric and electronic effects are involved, the former being related not only to the actual ground-state geometry but also to the steric hindrance toward excited-state distortion and exciplex formation.[27]

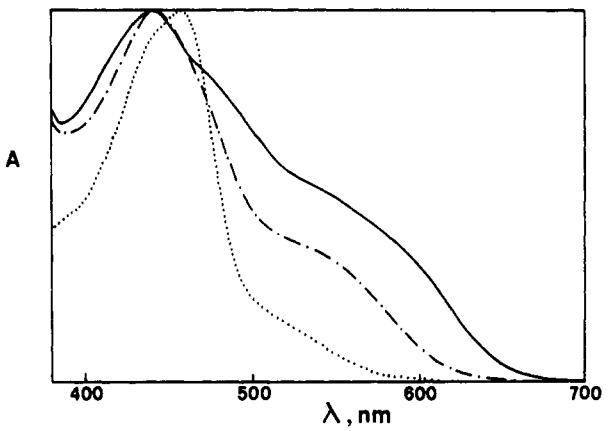

Figure 4. Normalized visible absorption spectra in CH_2Cl_2 (293 K) of $[Cu(dtp)_2]^+$ (—), $[Cu(2)_2]^+$ (-·-), and $[Cu(dmp)_2]^+$ (···).

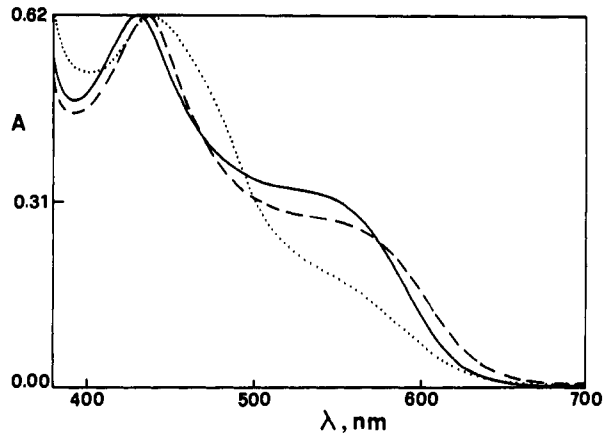

Figure 5. Visible absorption spectra in CH_2Cl_2 (10^{-4} M, 293 K) of $[Cu_2(k\text{-}84)]^{2+}$ (—), $[Cu_2(k\text{-}80)]^{2+}$ (– –), and $[Cu_2(k\text{-}82)]^{2+}$ (···).

(b) Absorption Spectra. A good model for the actual ligand units which are present in the knots and in their face-to-face isomers is 2-methyl-9-(*p*-anisyl)-1,10-phenanthroline (**2**). We have therefore investigated its spectroscopic and photophysical properties for comparison purposes.

The absorption spectra of the knots in the UV region, mainly due to ligand-centered transitions, are only slightly affected by the actual structure of each knot and are also very similar to those exhibited by the face-to-face compounds and by the model complex $[Cu(2)_2]^+$.

The visible absorption spectrum of the model compound $[Cu(2)_2]^+$ is shown in Figure 4. It is known that phenyl substituents in the 2,9-positions lower the absorptivity.[22] However, Figure 4 shows that if the spectral intensity is normalized at λ_{max} of band II, the $\lambda > 500$ nm tail (band I) of $[Cu(2)_2]^+$ is considerably more intense than that of $[Cu(dmp)_2]^+$ and less intense than that of $[Cu(dtp)_2]^+$ (dmp = 2,9-dimethyl-1,10-phenanthroline; dtp = 2,9-ditolyl-1,10-phenanthroline).[31] This shows that the intensity of band I relative to that of band II increases when phenyl substituents are present in the 2,9-positions. The MLCT bands I and II can clearly be seen for all the examined compounds, but each knot exhibits a distinct spectral profile (Figure 5).

Within an experimental error of ±10% (related to the small amount of sample weighed to prepare the solutions), the molar absorption coefficient at the maximum of the visible band (ϵ_{max}) is the same for all the knots and their isomeric face-to-face

(29) Parker, W. L.; Crosby, G. A. *J. Phys. Chem.* **1989**, *93*, 5692.
(30) Gordon, K. C.; McGarvey, J. J. *Inorg. Chem.* **1991**, *30*, 2986.
(31) Vögtle, F.; Lüer, I.; Balzani, V.; Armaroli, N. *Angew. Chem., Int. Ed. Engl.* **1991**, *30*, 1333.

Table II. Absorption Maxima and Luminescence Properties[a]

			298 K						77 K	
complex	z^b	x^c	λ_{max}^{abs} [d] (nm)	λ_{max}^{em} [d] (nm)	τ^d (ns)	$10^4\Phi^{em}$ [d]	$10^{-3}k_r^e$ (s^{-1})	$10^{-6}k_{nr}^f$ (s^{-1})	λ_{max}^{em} (nm)	τ^g (μs)
$[Cu_2(k\text{-}82)]^{2+}$	2	19	440	750	149	3.7	2.5	6.7	770	1.2
$[Cu_2(k\text{-}80)]^{2+}$	4	16	437	750	150	3.7	2.5	6.7	755	2.6
$[Cu_2(k\text{-}86)]^{2+}$	4	19	439	750	154	4.1	2.7	6.5	750	0.9[h]
$[Cu_2(k\text{-}84)]^{2+}$	6	16	431	742	208	7.2	3.5	4.8	750	0.9
$[Cu_2(k\text{-}90)]^{2+}$	6	19	434	742	174	5.5	3.2	5.7	755	1.2
$[Cu(2)_2]^{+}$			442	745	130	3.7	2.8	7.7	760	~0.5
$[Cu_2(m\text{-}43)_2]^{2+}$			436	745	170	5.3	3.1	5.9	730	2.3
$[Cu_2(m\text{-}45)_2]^{2+}$			437	745	171	5.5	3.2	5.8	740	2.7

[a] Solvent is CH_2Cl_2 unless otherwise noted. [b] Number of atoms of the aliphatic chain Z. [c] Number of atoms of the ether chain X. [d] Deaerated solutions. [e] Radiative decay rate constant. [f] Nonradiative decay rate constant. [g] CH_2Cl_2/CH_3OH (1:1, v/v). [h] A longer decay (τ = 2.6 μs) is also observed, presumably due to a small amount of $[Cu_2(m\text{-}43)_2]^{2+}$.

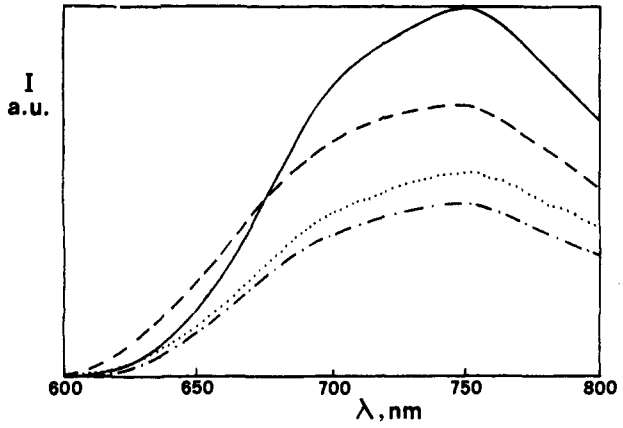

Figure 6. Corrected emission spectra in CH_2Cl_2 (λ_{exc} = 440 nm) of $[Cu_2(k\text{-}84)]^{2+}$ (—), $[Cu_2(m\text{-}43)_2]^{2+}$ (– –), $[Cu_2(k\text{-}86)]^{2+}$ (···), and $[Cu(2)_2]^{+}$ (—·—).

compounds (6200 M^{-1} cm^{-1}). In order to facilitate comparison, the visible spectra have therefore been displaced, taking the same value for ϵ_{max}. The spectra of $[Cu_2(k\text{-}82)]^{2+}$ and $[Cu_2(k\text{-}86)]^{2+}$ are similar to that of the $[Cu(2)_2]^{+}$ model compound, whereas the spectra of the other knots, and particularly that of $[Cu_2(k\text{-}84)]^{2+}$, are noticeably different (Figures 4–5, Table II).

Apparently, the lengths of the z and x chains that connect the phen-type ligands affect the "fine structure" of the coordination environment. In $[Cu_2(k\text{-}84)]^{2+}$, bands II and I seem to be better resolved, which suggests a more symmetric environment and/or a higher energy distortion frequency. It should also be noticed that, except in the case of $[Cu_2(k\text{-}82)]^{2+}$, in the spectra of the knots there is no evidence of additional shoulders compared with the spectrum of the mononuclear model compound $[Cu(2)_2]^{+}$. This shows that the two metal-containing units of each knot experience very similar (if not identical) geometrical environments. The spectrum of $[Cu_2(k\text{-}82)]^{2+}$, where the z connection is very short, seems to exhibit a broadening on the red side of bands I and II, but this could also be related to a higher distortion in each chromophoric group.

Finally, it is noteworthy that the spectra of the face-to-face isomers $[Cu_2(m\text{-}43)_2]^{2+}$ and $[Cu_2(m\text{-}45)_2]^{2+}$ are identical and very similar to those of the respective knots $[Cu_2(k\text{-}86)]^{2+}$ and $[Cu_2(k\text{-}90)]^{2+}$. This surprising result shows that the face-to-face and knotted situations offer very similar coordination environments to the metal ion.

(c) Luminescence Properties. The luminescent data and some related quantities have been collected in Table II. All the knots show a luminescence band in the red region of the spectrum that can straightforwardly be assigned to MLCT levels (Figure 6). As it happens, for previously investigated $[Cu(NN)_2]^{+}$ complexes, this band is very broad and weak and it becomes weaker, longer lived, and red-shifted in going from room temperature to 77 K. For example, for $[Cu_2(k\text{-}84)]^{2+}$, subtraction of the 77 K spectrum from the room-temperature spectrum suggests that in the latter there is a high-energy component whose maximum is at about 1500 cm^{-1} above the maximum of the low-temperature spectrum.

As we have seen above, this behavior is that generally observed for the $[Cu(NN)_2]^{+}$-type compounds and can be explained with the presence of a (higher energy) singlet and a (lower energy) triplet MLCT level in thermal equilibrium. The absorption and luminescence spectra show that there is a considerable Stokes shift (~4000 cm^{-1}) between absorption and emission from the $^1B_1$ MLCT level (for $[Cu_2(k\text{-}84)]^{2+}$, λ_{max}^{abs} ~ 540 nm (Figure 5) and λ_{max}^{em} ~ 742 nm (Figure 6)). This confirms that a strong distortion occurs in the MLCT excited states. From the spectrum at 77 K it is clear that the main contribution to the luminescence band comes from the ^{3}MLCT level even at high temperatures, as it is also shown by the values of k_r estimated from the Φ_{em}/τ ratios (Table II). Corrected excitation spectra show that the luminescent levels are reached with the same (presumably unitary) efficiency regardless of the excitation wavelength for all the compounds examined.

Within this general frame, we can notice that the luminescence properties of the various compounds are not identical. The main differences are as follows (Table II, Figure 6).

(i) At room temperature, the luminescence bands of $[Cu_2(k\text{-}84)]^{2+}$ and $[Cu_2(k\text{-}90)]^{2+}$ are blue-shifted, more intense, and longer lived compared with those of the other knots and of the model compound $[Cu(2)_2]^{+}$. Calculation of the radiative ($k_r = \Phi_{em}/\tau$) and nonradiative ($k_{nr} = 1/\tau$) rate constants also shows that $[Cu_2(k\text{-}84)]^{2+}$ and $[Cu_2(k\text{-}90)]^{2+}$ have larger k_r and smaller k_{nr} compared to those of the other knots. This suggests that $[Cu_2(k\text{-}84)]^{2+}$ and $[Cu_2(k\text{-}90)]^{2+}$ possess a more symmetric and more rigid structure than the other knots, in full agreement with the electrochemical results.

(ii) As in the case of the absorption spectra, the behavior of the $[Cu(2)_2]^{+}$ model compound is very similar to that of $[Cu_2(k\text{-}82)]^{2+}$, $[Cu_2(k\text{-}80)]^{2+}$, and $[Cu_2(k\text{-}86)]^{2+}$. It should also be noticed that the model compound exhibits the highest k_{nr} value, which is consistent with the high flexibility and/or easy accessibility to the metal center expected because the phen-type ligands are not incorporated into a macrocyclic structure.

(iii) At room temperature the behavior of the face-to-face $[Cu_2(m\text{-}43)_2]^{2+}$ and $[Cu_2(m\text{-}45)_2]^{2+}$ compounds is almost identical to that of the corresponding knots, but in going from room temperature to 77 K their bands become more intense and shift to higher energy and their lifetimes become much longer. This behavior is consistent with almost identical coordination spheres for knot and face-to-face isomers but suggests that the environments for the luminescent MLCT excited state are different in the two species, presumably because of the different positions of the connector units (and, as a consequence, of the solvent molecules) in the two isomers.

Finally, we note that the rate constant for the quenching of the luminescence by O_2 (Table III), obtained from the Stern–Volmer relationship

Table III. Stern–Volmer Rate Constants for the Quenching of the ^{3}MLCT Excited State in CH_2Cl_2 Solutions at 298 K

	$10^{-6}k_q[O_2]^a$ (s^{-1} M^{-1})	$10^{-6}k_q$[acetone]^b (s^{-1} M^{-1})
$[Cu_2(k\text{-}86)]^{2+}$	2.1	<0.1
$[Cu_2(k\text{-}84)]^{2+}$	2.1	<0.1
$[Cu(2)_2]^{+}$	1.7	1.0
$[Cu_2(m\text{-}43)_2]^{2+}$	2.0	0.2
$[Cu_2(m\text{-}45)_2]^{2+}$	2.3	0.2

[a] Quenching by O_2 in air-equilibrated solutions. [b] Quenching by 3 M acetone.

$$\tau^0/\tau = 1 + \tau^0 k_q[Q]$$

where τ^0 and τ are the luminescence lifetimes in the absence and presence of the quencher, respectively, is practically the same in all cases, including the model compound $[Cu(2)_2]^+$. This is an expected result since quenching by O_2 is likely due to an electron-transfer process from a ligand involved in the MLCT excited state, which is easily accessible to O_2. However, when the quenching process involves attack on the excited metal center to form exciplexes,[21,25] as in the case of acetone (Table III) or of coordinating counterions[25] (for $[Cu_2(k\text{-}84)]^{2+}$, the excited-state lifetime is the same for the BF_4^- and PF_6^- salts), the behavior of the model compound is very different from that of the knot and face-to-face structures, showing that the metal center is much less accessible when the **2**-type ligands are parts of knotted or cyclic strings.

Conclusions

We have prepared five new dicopper(I) knots and their face-to-face isomers. The preparation yields of the knots depend strongly on the length of the methylene fragment which links the two chelating units and the length of the poly(ethyleneoxy) units used in the cyclization step. In several cases the face-to-face compounds were obtained as the major product. The electrochemical behavior of the prepared compounds also depends on their intimate structure, imposed by the length of the two linkers. The most stable compound toward Cu(I) oxidation is the 84-membered knotted one. In CH_2Cl_2 solution, the Cu_2 knots and their face-to-face isomers exhibit MLCT absorption bands in the visible spectral region and MLCT luminescence in the 700–750-nm region, as expected for $[Cu(NN)_2]^+$-type chromophoric units. Most of the luminescence comes from the lowest ^{3}MLCT level, but a ^{1}MLCT level also contributes to the room-temperature emission. Closer examination shows that the absorption profile and the properties of the luminescent ^{3}MLCT level depend on the lengths of the z and x connectors (Figure 3), which is likely to affect the detailed ground-state geometry and the excited-state distortion. In fact, for several absorption and luminescence (or luminescence-related) properties (namely, λ_{max}^{abs} of band II, ϵ_{max} of band I, λ_{max}^{em} k_r, k_{nr}, and k_q(acetone)), the knots can be ordered in series where the two extremes are $[Cu_2(k\text{-}84)]^{2+}$ and $[Cu_2(k\text{-}82)]^{2+}$, the former being the most rigid and the one in which Cu(I) is best shielded, as indicated by electrochemistry. This shows that the length of the (shorter) z connection plays an important role in determining the "fine structure" of the geometrical arrangement.

Experimental Section

General Procedures. Commercial 1,10-phenanthroline monohydrate was dried before use by three successive azeotropic distillations (51 mL of toluene and 35 mL of absolute ethanol) and subsequent drying over P_2O_5 in a vacuum. Neat 1,4-dichlorobutane and 1,6-dichlorohexane as well as *p*-bromoanisole were purified and dried by filtration through an aluminum oxide 90 column (activity grade II–III), and then collected and stored under argon. All other chemicals were of the best commercially available grade and were used without further purification. ^{1}H-NMR spectra were recordered with a Bruker WP 200SY spectrometer. Mass spectra were obtained on a ZAB-HF spectrometer (FAB). Melting points were measured with a Büchi SMP20 apparatus (uncorrected).

Preparation of 2-(*p*-Anisyl)-1,10-phenanthroline (1). *p*-Anisyllithium was prepared by the direct interaction of freshly cut lithium (6 g, 0.9 mol) with *p*-bromoanisole (41.8 g, 224 mmol) in ether (180 mL) under argon and at room temperature[10] and titrated.[32] A 150 mL portion of the 1.05 M *p*-anisyllithium solution thus obtained was slowly added by means of a double-ended needle to a degassed suspension of 11.0 g (61.1 mmol) of 1,10-phenanthroline in 250 mL of anhydrous ether kept at 0 °C. After the resulting dark red solution was stirred for 4 h under argon at 7 °C, it was hydrolyzed with water at 0 °C. The bright yellow ether layer was decanted and the aqueous layer extracted three times with 200 mL portions of CH_2Cl_2. The combined organic layers were thereafter rearomatized by successive additions of MnO_2 under effective magnetic stirring (MnO_2 Merck No. 805958, ~20 g for each batch). This reoxidation, easily followed by TLC and the disappearance of the yellow color, was ended after the addition of 120 g of MnO_2. After the mixture was dried over $MgSO_4$, the black slurry could be easily filtered on a sintered glass and the filtrate evaporated to dryness to give 31.8 g of crude **1**. Column chromatography on silica gel (eluent CH_2Cl_2 containing 1% MeOH) and recrystallization from hot toluene yielded 12.1 g (42.3 mmol, 69% yield) of pure **1** as colorless needles (mp 178 °C). ^{1}H NMR ($CDCl_3$): δ 9.27 (dd, 1H, H_9, $J_1 \sim 4.5$ Hz, $J_2 \sim 1.8$ Hz), 8.37 (d, 2H, H_o, $J \sim 8.9$ Hz), 8.29 (dd, 1H, H_7, $J_1 \sim 8.1$ Hz, $J_2 \sim 1.8$ Hz), 8.28 (d, 1H, H_4, $J \sim 8.4$ Hz), 8.08 (d, 1H, H_3, $J \sim 8.4$ Hz), 7.79 (AB, 2H, $H_{5,6}$, $J \sim 8.9$ Hz), 7.66 (dd, 1H, H_8, $J_1 \sim 8.1$ Hz, $J_2 \sim 4.5$ Hz), 7.07 (d, 2H, H_m, $J \sim 8.9$ Hz), 3.90 (s, 3H, OCH_3). Anal. Calcd for $C_{19}H_{14}N_2O$: C, 79.70; H, 4.93. Found: C, 79.75; H, 4.97.

Preparation of 2-Methyl-9-(*p*-anisyl)-1,10-phenanthroline (2). A 30 mL portion of a 1.57 M methyllithium solution was slowly added by a syringe to a degassed suspension of 8.2 g (28.7 mmol) of **1** in 250 mL of anhydrous ether kept at 0 °C. After the resulting dark red solution was stirred for 6 h under argon at 0–10 °C, it was hydrolyzed with water at 0 °C. The bright yellow ether layer was decanted and the aqueous layer extracted three times with 100 mL portions of CH_2Cl_2. The combined organic layers were thereafter rearomatized with MnO_2 (90 g), dried over $MgSO_4$, and filtered on a sintered glass; the filtrate was then evaporated to dryness to give 8.7 g of crude **2**. Column chromatography on silica gel (eluent CH_2Cl_2) yielded 7.9 g (26.3 mmol, 92% yield) of pure **2** as colorless needles (mp 161 °C). ^{1}H NMR ($CDCl_3$): δ 8.39 (d, 2H, H_o, $J \sim 8.9$ Hz), 8.27 (d, 1H, H_7, $J \sim 8.5$ Hz), 8.17 (d, 1H, H_4, $J \sim 8.2$ Hz), 8.07 (d, 1H, H_8, $J \sim 8.5$ Hz), 7.74 (AB, 2H, $H_{5,6}$, $J \sim 8.9$ Hz), 7.53 (d, 1H, H_3, $J \sim 8.2$ Hz), 7.08 (d, 2H, H_m, $J \sim 8.9$ Hz), 3.91 (s, 3H, OCH_3), 3.00 (s, 3H, CH_3). Anal. Calcd for $C_{20}H_{16}N_2O$: C, 79.98; H, 5.37; N, 9.33. Found: C, 79.88; H, 5.33; N, 9.01.

Preparation of Bis(phenanthroline) 3. A freshly prepared solution of LDA (26.4 mmol) in THF was slowly added by means of a double-ended needle to a degassed solution of 7.2 g (24 mmol) of **2** in 250 mL of anhydrous THF kept at –78 °C. After the resulting deep purple solution was stirred for 3 h under argon at –78 °C, a solution of iodine (6.1 g, 24 mmol) in THF (60 mL) was added dropwise over 30 min. Stirring was continued for a further 3 h at –78 °C. After the temperature was raised to 0 °C, the resulting yellow suspension was hydrolyzed with water. The yellow precipitated solid was filtered out onto paper, washed with THF, and dried (high vacuum in the presence of P_2O_5) to give crude **3**. The latter was adsorbed on alumina and purified by column chromatography on silica gel (eluent CH_2Cl_2 containing 3% MeOH), giving pure **3** (5.55 g, 9.3 mmol, 77% yield) as a colorless solid (mp >260 °C dec). ^{1}H NMR (CF_3CO_2D): δ 9.28 (d, 2H, H_7, $J \sim 8.7$ Hz), 9.24 (d, 2H, H_4, $J \sim 8.5$ Hz), 8.68 (d, 2H, H_8, $J \sim 8.7$ Hz), 8.55 (AB, 4H, $H_{5,6}$, $J \sim 8.9$ Hz), 8.51 (d, 2H, H_3, $J \sim 8.5$ Hz), 8.23 (d, 4H, H_o, $J \sim 8.9$ Hz), 7.38 (d, 4H, H_m, $J \sim 8.9$ Hz), 4.34 (s, 4H, CH_2), 4.11 (s, 6H, OCH_3). Anal. Calcd for $C_{40}H_{30}N_4O_2 \cdot H_2O$: C, 77.90; H, 5.23; N, 9.08. Found: C, 77.74; H, 5.00; N, 8.79. FAB-MS: m/z found 599.2 (MH^+), calcd 599.7.

Preparation of Bis(phenanthroline) 4. This compound was prepared as described by ref 7.

Preparation of Bis(phenanthroline) 5. 1,6-Dilithiohexane was prepared by direct interaction between freshly prepared lithium sand (1.73 g, 250 mmol) and 1,6-dichlorobutane (7.25 mL, 50 mmol) in anhydrous ether (75 mL) under argon at 0 °C.[11] The resulting organolithium compound appeared as a white-gray solid suspended in the ether and could not be titrated. The latter suspension was slowly added by means of a double-

(32) Gilman, H.; Cartledge, F. K. *J. Organomet. Chem.* **1964**, *2*, 447.

Table IV. Demethylation of **3–5**

		substrate			diphenol				
pyridine (mL)	HCl (mL)	no.	W (g)	mmol	no.	W (g)	mmol	characterization	yield (%)
8.0	8.8	3	2.00	3.34	6	1.89	3.31	beige solid; mp > 282 °C Anal. Calcd for $C_{38}H_{26}N_4O_2 \cdot 2MeOH$: C, 75.69; H, 5.40; N, 8.82 Found: C, 75.75; H, 5.14; N, 8.60.	99
13.0	14.3	4	1.25	2.00	7	0.96	1.60	pink solid; mp > 282 °C Anal. Calcd for $C_{40}H_{30}N_4O_2$: C, 80.25; H, 5.05; N, 9.36. Found: C, 80.17; H, 5.07; N, 9.20.	80
18.9	20.8	5	1.90	2.90	8	1.58	2.53	pink-beige solid; mp > 282 °C Anal.: Nonreproducible results.	87

Table V. ^{1}H-NMR Chemical Shifts (ppm) for Diphenols **6–8**

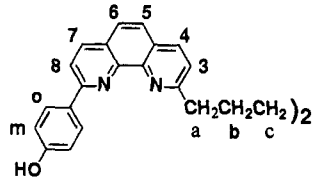

diphenol	OH	H_3	H_4	$H_{5,6}$	H_7	H_8	H_o	H_m	CH_2-a	CH_2-b	CH_2-c
6	9.83	7.83	8.34	7.89	8.46	8.25	8.33	6.96	3.82		
(DMSO)	s, 2H	d, 2H	d, 2H	AB, 4H	d, 2H	d, 2H	d, 4H	d, 4H	s, 4H		
7	10.21	7.87	8.48	8.02	8.38	8.59	8.51	7.17	3.44	2.27	
(DMF, CD_2Cl_2)	s, 2H	d, 2H	d, 2H	AB, 4H	d, 2H	d, 2H	d, 4H	d, 4H	m, 4H	m, 4H	
8	9.82	7.60	8.30	7.84	8.41	8.19	8.27	6.95	3.12	1.95	1.59
(DMSO, CD_2Cl_2)	s, 2H	d, 2H	d, 2H	AB, 4H	d, 2H	d, 2H	d, 4H	d, 4H	t, 4H	m, 4H	m, 4H

ended needle to a degassed suspension of **1** (3.00 g, 10.49 mmol) in 100 mL of anhydrous ether maintained at 0 °C. The mixture rapidly turned dark red. After complete addition of $Li(CH_2)_6Li$ (1 h), the resulting solution was kept stirring and allowed to reach room temperature overnight. It was then hydrolyzed at low temperature (−5 °C) with water. The bright yellow ether layer was decanted and the aqueous layer extracted three times with CH_2Cl_2. The combined organic layers were rearomatized with MnO_2 (40 g). After the mixture was dried over $MgSO_4$, the black slurry was filtered on a sintered glass and the filtrate evaporated to dryness to give 4.08 g of crude **5** (quantitative yield). Column chromatography on silica gel eluted with CH_2Cl_2 and 2–4% MeOH yielded 2.070 g (3.16 mmol, 60% yield) of pure **5** as a pale yellow solid (mp 194–195 °C). ^{1}H NMR (CD_2Cl_2): δ 8.30 (d, 4H, H_o, $J \sim 8.9$ Hz), 8.24 (d, 2H, H_7, $J \sim 8.6$ Hz), 8.13 (d, 2H, H_4, $J \sim 8.2$ Hz), 8.03 (d, 2H, H_8, $J \sim 8.5$ Hz), 7.71 (s, 4H, H_5 and H_6), 7.52 (d, 2H, H_3, $J \sim 8.2$ Hz), 7.07 (d, 4H, H_m, $J \sim 8.9$ Hz), 3.86 (s, 6H, OCH_3), 3.21 (t, 4H, H_a), 2.01 (m, 4H, H_b), 1.66 (m, 4H, H_c). Anal. Calcd for $C_{44}H_{38}N_4O_2 \cdot H_2O$: C, 78.54; H, 5.99. Found: C, 78.78; H, 5.81.

Preparation of the Diphenols 6–8.[12] The general procedure used to prepare **6–8** was the following: technical grade pyridine was poured into a 100 mL three-necked flask fitted with a thermometer and a magnetic stirrer. Under rapid stirring, concentrated hydrochloric acid was added. The flask was equipped for distillation, and water was distilled from the mixture until its internal temperature rose to 210 °C. After being cooled to ~140 °C, the bis(phenanthroline) **3**, **4**, or **5** was added at once as a solid and the reaction flask was fitted with a reflux condenser connected to a source of argon. The mixture was stirred and refluxed for 3 h (190 < T < 200 °C). The hot reaction mixture was then diluted with ~20 mL of warm water and slowly poured into ~50 mL of hot water. The crude acidic diphenol **6–8** suspended in an ethanol/water mixture (100:60 mL) was neutralized with a dilute NaOH solution. After this pH-monitored neutralization (endpoint pH = 7.3), the suspension was diluted with more hot water (~300 mL). Neutral diphenols precipitated during cooling. They were filtered out onto paper, washed with cold water, air-dried, and further dried under high vacuum in the presence of P_2O_5. Such products could be used without other purification. Amounts of used reactants, yields, and characterization of diphenols **6–8** are given in Table IV and V.

Preparation of the Acyclic Precursors 9^{2+}–14^{2+}. All these compounds were prepared by the double-ended needle transfer technique. $Cu(CH_3CN)_4 \cdot BF_4$ or $Cu(CH_3CN)_4 \cdot PF_6$ were dissolved in degassed CH_3CN and added under argon at room temperature to a stirred degassed solution of the diphenol in DMF. The mixtures turned dark red instantaneously, indicating the formation of the complexes 9^{2+}–14^{2+}. After the solution was stirred for 4 h under argon at room temperature, the solvents were evaporated to dryness and dark red solids of crude (9^{2+}, 12^{2+}), (10^{2+}, 13^{2+}), and (11^{2+}, 14^{2+}) were obtained in quantitative yields. The two types of complexes (helical and nonhelical) are in equilibrium and exhibit the same color and R_f. Therefore, they could not be isolated and fully characterized. They were used as crude mixtures without further purification. Precise experimental conditions are collected in Table VI.

Table VI. Preparation of the Acyclic Precursors 9^{2+}–14^{2+}

diphenol in DMF				$Cu(CH_3CN)_4 \cdot BF_4$ in CH_3CN			isolated complexes		
no.	W (g)	mmol	mL	W (g)	mmol	mL	no.	W (g)	mmol
6	0.900	1.58	200	0.496	1.58	100	(9^{2+}, 12^{2+})	1.14	0.79
7	1.130	1.89	50	0.653	2.08	60	(10^{2+}, 13^{2+})	1.41	0.94
8	1.252	2.00	50	0.693	2.20	70	(11^{2+}, 14^{2+})	1.56	1.00

Cyclization Affording $[Cu_2(k\text{-}80)]^{2+}$ to $[Cu_2(k\text{-}90)]^{2+}$ and $[Cu_2(m\text{-}40)_2]^{2+}$ to $[Cu_2(m\text{-}45)_2]^{2+}$. General procedure: A mixture of 1 equiv of the acyclic Cu(I) complexes and 2 equiv of the diiodo derivative of hexa- or pentaethylene glycol in DMF was added dropwise under efficient stirring to an argon-flushed suspension of Cs_2CO_3 in DMF kept at 60–62 °C. The mixture, first orange-yellow, turned progressively dark brown-red. The reaction was monitored by TLC, which showed that the poly(oxyethylene) chain was consumed faster than the Cu(I) complexes. A supplementary chain in DMF was added within a few hours. After this second addition, stirring and heating were continued for several hours. DMF was then evaporated and the dry dark red residue taken up in $CH_2Cl_2 \cdot H_2O$. The aqueous layer was extracted three times with CH_2Cl_2. After decantation and discarding of the brown insoluble compounds (oligomers) appearing between both phases, the remaining dark red CH_2Cl_2 layer was washed twice with water and thereafter treated overnight with a large excess of $NaBF_4$ (or KPF_6) in a minimum amount of water. By means of this exchange reaction, we obtained the cyclic Cu(I) complexes, originally formed as carbonates, iodides, and tetrafluoroborates (or hexafluorophosphates), exclusively as their BF_4^- or PF_6^- salts. The resulting organic layer, washed twice with water, was dried over $MgSO_4$ and evaporated to dryness to yield a dark red solid. Several successive chromatographies on silica gel (eluent CH_2Cl_2 containing 1–6% MeOH) were necessary to yield pure knots and pure face-to-face complexes. Precise experimental conditions and characterizations of the isolated complexes are given in Tables VII–IX. All these complexes are dark red solids (mp > 280 °C).

Electrochemical Measurements. (a) Solvents and Supporting Electrolytes. CH_3CN, spectroscopic grade, was distilled over CaH_2 under argon and stored under argon. $LiClO_4$ was dried for 24 h at 80 °C in an oven.

(b) Instrumentation. A Bruker EI 30M potentiostat and an Ifelec IF 3802 recorder served for cyclic voltammetry measurements. A saturated calomel electrode (SCE) served as the reference electrode. It was separated from the test solution by an auxiliary compartment filled with

Table VII. Preparation of $[Cu_2(k\text{-}80)]^{2+}$ to $[Cu_2(k\text{-}90)]^{2+}$ and $[Cu_2(m\text{-}40)_2]^{2+}$ to $[Cu_2(m\text{-}45)_2]^{2+}$

acyclic precursor and chain fragment in DMF				Cs_2CO_3 in DMF			addition	2nd add. of chain			overall	isolated complexes		
no.	W (g)	mmol		W (g)	mmol	mL	W (g)	mmol	mL	(h)	W (g)	mmol	time (h)	no.	W (mg)	yield(%)
(9^{2+}, 12^{2+})	1.24	0.86	hexa	0.95	1.9	180	1.9	6.0	300	18	0.30	0.60	36	$[Cu_2(m\text{-}41)_2]^{2+}$	8	0.5
														$[Cu_2(k\text{-}82)]^{2+}$	8	0.5
(10^{2+}, 13^{2+})	1.61	1.00	penta	1.01	2.2	200	2.5	7.7	350	23	0.28	0.60	41	$[Cu_2(m\text{-}40)_2]^{2+}$	88	4.6
														$[Cu_2(k\text{-}80)]^{2+}$	14	0.7
(10^{2+}, 13^{2+})[b]	1.41	0.94	hexa	1.04	2.1	200	3.5	10.7	400	21	0.45	0.89	47	$[Cu_2(m\text{-}43)_2]^{2+}$	457	24
														$[Cu_2(k\text{-}86)]^{2+}$	57	3
(11^{2+}, 14^{2+})	0.75	0.45	penta	0.45	1.0	100	1.5	4.6	400	20	0.45	0.98	42	$[Cu_2(m\text{-}42)_2]^{2+}$		[a]
														$[Cu_2(k\text{-}84)]^{2+}$	75	8
(11^{2+}, 14^{2+})	1.56	1.0	hexa	1.12	2.2	200	3.8	11.6	400	23	0.33	0.66	48	$[Cu_2(m\text{-}45)_2]^{2+}$	429	21
														$[Cu_2(k\text{-}90)]^{2+}$	51	2.5

[a] $[Cu_2(m\text{-}42)_2]^{2+}$ is unstable and decomposes on the silica gel column. It could only be characterized by NMR (addition of Cu(I) salt to m-42 in the NMR tube). [b] See ref 7.

Table VIII. ^{1}H-NMR (at 25 °C in $CHDCl_2$, δ(H) = 5.32 ppm) and Mass Spectra Characterizations of the Various Knots

	NMR[a]											MS (FAB)	
	aromatic region							small linker					
knot	H_3	H_4	$H_{5,6}$	H_7	H_8	H_o	H_m	$H_{a/a'}$	$H_{b/b'}$	$H_{c/c'}$	mol wt	$[(Cu_2(k)\cdot BF_4]^+$ (or PF_6)	M/2 for $[Cu_2(k)]^{2+}$
$[Cu_2(k\text{-}82)]\cdot 2BF_4$	6.41	7.35	7.93	8.75	8.05	7.34	5.94	2.13			1934.6	calcd 1847.8	880.5
								1.77				found 1847.3	880.1
$[Cu_2(k\text{-}80)]\cdot 2BF_4$	6.28	8.27	8.17	8.71	8.09	7.32	5.71	1.57	0.19		1902.6	calcd 1815.8	864.5
								1.46				found 1815.5	864.2
$[Cu_2(k\text{-}86)]\cdot 2BF_4$	6.54	8.23	8.15	8.66	7.99	7.19	5.77	1.90	0.70		1990.7	calcd 1903.9	908.5
								1.60	0.50			found 1903.8	908.2
$[Cu_2(k\text{-}84)]\cdot 2PF_6$	6.74	8.51	8.08	8.63	8.03	7.29	5.73	1.87	–0.04	–0.50	2073.1	calcd 1928.2	891.6
								1.46		–0.89		found 1928.6	891.3
$[Cu_2(k\text{-}90)]\cdot 2BF_4$	6.87	8.47	8.10	8.63	8.02	7.29	5.79	1.78	0.18	–0.37	2045.2	calcd 1958.2	935.6
								1.65	–0.09			found 1958.4	935.2

[a] All dicopper(I) trefoil knots showed a similar highly characteristic pattern: an AB pattern for H_3 or H_7 and H_4 or H_8 ($J \sim 8.5$ Hz); an AB pattern or a singlet for H_5 and H_6 ($J \sim 8.9$ Hz); an AA'XX' system for H_o and H_m ($J \sim 8.7$ Hz); multiplets for $H_{a/a'}$, $H_{b/b'}$, and $H_{c/c'}$; a broad multiplet between 3.0 and 4.0 ppm for the poly(oxyethylene) chains.

Table IX. ^{1}H-NMR (at 25 °C in $CHDCl_2$, δ(H) = 5.32 ppm) and Mass Spectra Characterizations of the Various Face-to-Face Complexes

	NMR[a]											MS (FAB)	
	aromatic region							small linker					
complex	H_3	H_4	$H_{5,6}$	H_7	H_8	H_o	H_m	$H_{a/a'}$	$H_{b/b'}$	$H_{c/c'}$	mol wt	$[Cu_2(m)_2\cdot BF_4]^+$	$[Cu(m)]^+$
$[Cu_2(m\text{-}41)_2]\cdot 2BF_4$	7.70	8.40	7.89	8.69	7.97	6.79	5.94	3.40			1934.6	calcd 1847.8	880.5
												found 1847.1	879.1
$[Cu_2(m\text{-}40)_2]\cdot 2BF_4$	7.21	8.55	8.00	8.59	7.92	7.03	5.76	2.24	1.05		1902.6	calcd 1815.8	864.5
									0.94			found 1815.4	863.2
$[Cu_2(m\text{-}43)_2]\cdot 2BF_4$	7.37	8.59	8.02	8.52	7.84	6.94	5.76	2.54	1.30		1990.7	calcd 1903.9	908.5
									1.20			found 1903.7	907.8
$[Cu_2(m\text{-}42)_2]\cdot 2BF_4$	7.21	8.43	8.04	8.57	7.94	7.08	5.82	2.16	1.02	0.46	[b]	[b]	[b]
$[Cu_2(m\text{-}45)_2]\cdot 2BF_4$	7.28	8.45	8.04	8.58	7.93	7.07	5.76	2.34	1.16	0.60	2045.2	calcd 1958.2	935.6
												found 1958.5	935.2

[a] All face-to-face complexes exhibit a highly characteristic pattern which is almost analogous to that observed for the dicopper(I) trefoil knots. [b] Unstable and could not be isolated.

a 10^{-1} M solution of $Et_4N^+BF_4^-$ in CH_3CN. The working electrode was a planar platinum one. All experiments were done under an argon atmosphere in a Metrohm universal recipient, in a three-electrode configuration.

Absorption and Luminescence Measurements. The solvent used for the absorption spectra and luminescence studies was CH_2Cl_2 (Merck, pro analysi). The absorption spectra were recorded with a Perkin-Elmer λ6 spectrophotometer. Corrected emission and excitation spectra were obtained with a Perkin-Elmer LS-50 spectrofluorimeter. Luminescence quantum yields were measured with a Perkin-Elmer 650-40 spectrofluorimeter, following the method described by Demas and Crosby[33] (the standard used was $Os(bpy)_3^{2+}$ in CH_3CN; $\Phi = 5.0 \times 10^{-3}$).[34] Luminescence lifetimes were obtained with an Edinburgh single-photon counting apparatus (N_2 lamp, 337 nm). For the luminescence measurements at room temperature, the solutions were deaerated by at least four freeze–pump–thaw cycles. Experimental uncertainties: λ^{abs}, 2 nm; λ^{em}, 5 nm; τ, 10%; Φ^{em}, 20%.

Acknowledgments. We thank the CNRS and the Italian Ministry of the Universities and Scientific Research for financial support and the French Ministry of Research and Space for a fellowship (J.-F.N.). We also thank P. Maltèse for high-field NMR spectra, the Mass-spectrometry group for MS measurements, and Dr. J.-M. Kern for his help in electrochemical measurements.

(33) Demas, J. N.; Crosby, G. A. *J. Phys. Chem.* **1971**, *75*, 991.

(34) Kober, E. M.; Caspar, J. V.; Lumpkim, R. S.; Meyer, T. J. *J. Phys. Chem.* **1986**, *90*, 3722.